Two-phase flow pattern recognition in a varying section based on void fraction and pressure measurements

Two-phase flow pattern recognition in a varying section based on void fraction and pressure measurements.

F. de Kerret, I. Benito, C. Béguin, D. Pelletier and S. Etienne
Polytechnique Montréal, 2900 boul. Édouard-Montpetit, Montréal, QC H3T 1J4, Canada
E-mail: stephane.etienne@polymtl.ca

Abstract. In a hydroelectric turbine, the air injected during operation has an impact on the yield of the machine leading to important losses of energy. To understand those losses and be able to reduce them, a first step is to understand the pattern of the two-phase flows and describe their characteristics in the turbine. Those two-phase flows can be bubbly, intermittent, or annular, with different types of intermittent flow possible. Two-phase flow patterns are well defined in classical geometries such as cylinders with reliable descriptions available [5]. But, there is a critical lack of knowledge for flow patterns in other geometries. In our present work we take interest into a geometry that is a pipe with periodical changes of the section and realize a flow pattern map. To realize this map, we measure the pressure variations and void fraction fluctuations while changing the flow rates of water and air in our test section. We then use our physical understanding of the phenomena to analyze data and identify different flow patterns, characterize them, and build a new flow pattern map.

1. Introduction

Increasing the yield of hydroelectric turbines is a key issue especially in Quebec, where 97% of the electricity is hydroelectric. The air injected during operation decreases turbine's efficiency and also results in pressure fluctuations that can affect the turbine's lifespan. Hence the yield can be improved through a better understanding of the two phase flow behavior over the turbine when air is injected. Beyond this importance for hydroelectric turbines, the understanding of two phase flow is essential for numerous processes in the petroleum, chemical and nuclear realms. Indeed two phase flows can generate important forces on structures, which can lead to dramatic consequences as in the San Onofre nuclear plant accident [2].

Two phase flows were first studied in cylindrical pipes, as it is the most current geometry, and different flow patterns identified. Depending on the two fluids flow rates, their characteristics, and the diameter of the pipe, the patterns differ. From a pure flow of air, when the liquid flow rate is increased, the flow goes from "annular" (a), with a liquid film along the side wall and drops entrained in the gas flow to "churn" (b) with chaotic structures and oscillatory motions, then to "slug" (c) with bullet shaped structures of gas in water, and finally to "bubbly" (d) with bubbles in a continuum of water, as shown on Fig. 1. In the case of a jet of air in water, the flow will necessarily go through these patterns since pure air is injected, and far from the injection bubbles are present. [3]

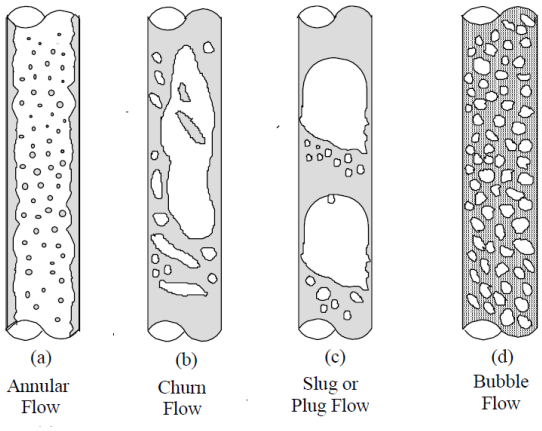

Figure 1: Flow pattern in vertical upward flow in cylinders.[4].

The flow pattern maps in cylinders are well documented and results are reliable [5–7]. The classical map by Taitel *et. al* (1980) is shown in Fig. 2a for a diameter of 3 cm. However, for other geometries, much work remains to be done. The most studied non cylindrical geometry is a tube bundle which represents the upper part of nuclear steam generators. In this geometry, it is more difficult to identify differences between flow patterns and usually only three patterns are defined: bubbly, intermittent, and annular. Intermittent patterns regroup slug and churn flows. After the first map based on visual observations [8], only few groups used objective parameters to segregate the different patterns. Noghrehkar *et al.* (1999) [1] relied on void fraction measurements. They analyzed, as explained below, the probability density function (PDF) of the void fraction for each experimental condition, and used it to sort out flow patterns. Ulbrich and Mewes [9] measured and analyzed pressure fluctuations to identify the different flow patterns. Their criterion is based on the fact that the intermittent flow is characterized by pressure fluctuations. Those two studies give very different results as one can see on Fig. 2b.
In the following work we present both pressure fluctuations and void fraction variations to characterize flow patterns and create a more detailed flow pattern map. Visual observations are often difficult, since we can't see what is happening inside the bundle. The geometry we study here is meant to represent the typical configuration for a nuclear plant steam generator, but the methodology we use can be applied to all geometries.

2. Experimental setup

Tests are carried out in a two meters long test section shown on Fig. 3. The geometry aims at representing the upper part of a steam generator. In this part two phase flow goes through a perpendicular tube bundle. For practical reasons experiments have been handled in a part of the tube bundle, with half tubes instead of a full tube bundle. The diameter of our tubes is $D = 38\ mm$ which is about twice as much as the diameters used in the industry. This choice was made so that we have room to insert an optical probe. More information about the test section is available in Mureithi and Masabarakiza (2011) [10].

A custom-made optical probe gives local information about the nature of the fluid at a frequency of 50 000 Hz. Optical probes work with the following principle: a laser beam goes into an optical fiber in the probe installed in the flow. As optical index of water is higher than optical index of air, the beam will be mostly reflected when the fiber is in air, and will mostly exit when it is in water. The returning signal is analyzed and gives information on the local structures. Measurements are done only in one location in the center of the flow. More

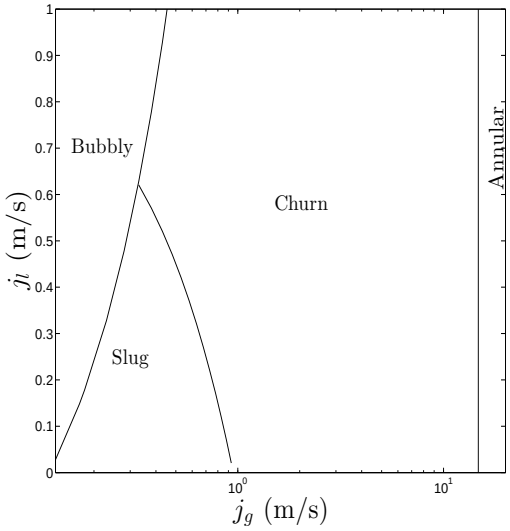

(a) Flow pattern map in a 3 cm diameter pipe.

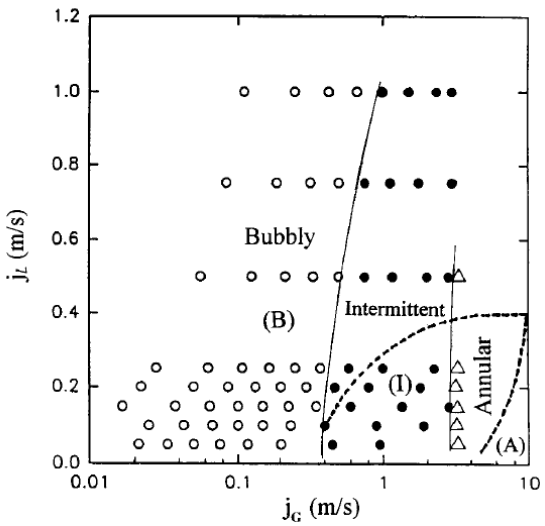

(b) Flow pattern map realized by Noghrehkar et. al (1999) in a bundle with tubes diameter of 1.27 cm, with the borders from Ulbrich and Mewes (1994) in doted line in a bundle with tubes diameter of 2.00 cm.

Figure 2

information is available on optical probes in the literature [11, 12]. Pressure measurements have been sampled at a frequency of 1000 Hz, at three locations in the experimental setup. Locations 2 and 3 are used to measure pressure fluctuations. Entrance pressure measurement is only meant to give a better estimate of the pressure drop. Water and gas are injected at the bottom of the test section. Water flows in the experimental setup in a closed loop, thanks to a gear pump previously calibrated. Gas comes from the "Polytechnique Montréal" pressurized air circuit. Air flow rate is measured by means of an orifice plate.

3. Notations

In our experimental setup we vary the water and air volumetric flow rate, Q_l and Q_g. In addition to those two parameters we define:

- P the pitch length,
- D the diameter,
- $L = 10$ cm the depth of the test section,
- $(P - D)L$ the typical area of the test section [11],
- β the volumetric quality with $\beta = \dfrac{Q_g}{Q_g + Q_l}$,
- j_g the gas superficial velocity $j_g = \dfrac{Q_g}{(P-D)L} = \beta U$,
- j_l the liquid superficial velocity $j_l = \dfrac{Q_l}{(P-D)L} = (1-\beta)U$,
- U the homogeneous velocity with $U = j_g + j_l$.

Superficial velocities are velocities each flow would have if it were the only fluid. The homogeneous velocity is the velocity the flow would have if both fluids had the same velocity.

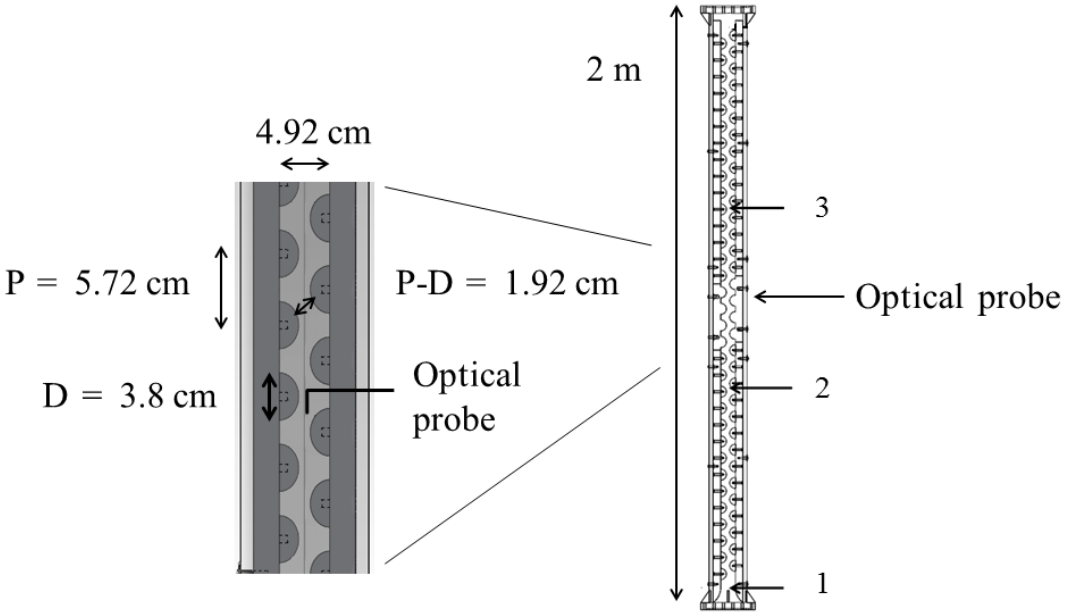

Figure 3: Mock up of the experimental setup.

4. Post-processing

To efficiently sort out patterns, pressure Fourier transform and void fraction probability density function (PDF) were extracted.

4.1. Probability density function of void fraction

χ_g is the indicator function with χ_g=1 if the probe is in gas and χ_g=0 if it is in liquid. Void indicator function is measured locally at a 50 KHz frequency. To create the PDF one has to calculate the mean void fraction measured during a time T_s called sampling time. Void fraction is defined as:

$$\varepsilon(t) = \frac{1}{T_S} \int_{t-\frac{T_s}{2}}^{t+\frac{T_s}{2}} \chi_g(\tau)\, \mathrm{d}\tau \tag{1}$$

Those mean void fractions allow to calculate the probability density function defined as:

$$P(a \leq \varepsilon \leq b) = \int_a^b PDF(\varepsilon)\, \mathrm{d}\varepsilon \tag{2}$$

Where a and b are two values of ε. One example of PDF is plotted on Fig. 4a, for which there is a probability of 0.14 that the void fraction be between $\varepsilon = 99\%$ and $\varepsilon = 100\%$ during a sampling time. This sampling time is important since two PDFs of the same signal χ_g(t) with different sampling times will be different. The sampling length is calculated based on the sampling time and the homogeneous velocity U. It is the length of flow analyzed that goes across the probe during the sampling time. This sampling length L_s allows the experimentalist to adjust to two phase flow structures. For example if the sampling length is 1 mm, a peak at a

void fraction $\varepsilon = 0\%$ allows to conclude that the flow carries water structures larger than 1 mm. Since the sampling length depends on the velocity, the number of measurement points during this length will decrease as the velocity increases. The void fraction precision will be adapted consequently.
An issue with the methodology used by Noghrehkar *et al.* is that they calculate their PDF with a fixed sampling time. The consequence is that the sampling length they use depends on the velocity, resulting in a bias in their analysis. For example when they are supposed to study annular flows, their sampling length is $L_s = 4\ cm$ which is higher than any interesting structure. This sampling length only results in giving the averaged void fraction in the flow.

4.2. Pressure Fourier transform
The pressure Fourier transform is calculated using several Hanning windows of 12 seconds with a 75% overlap. The Fourier transform is calculated on a total duration of 60 seconds. A typical example is shown on Fig. 7 for which important fluctuations of pressure around 5Hz can be observed.

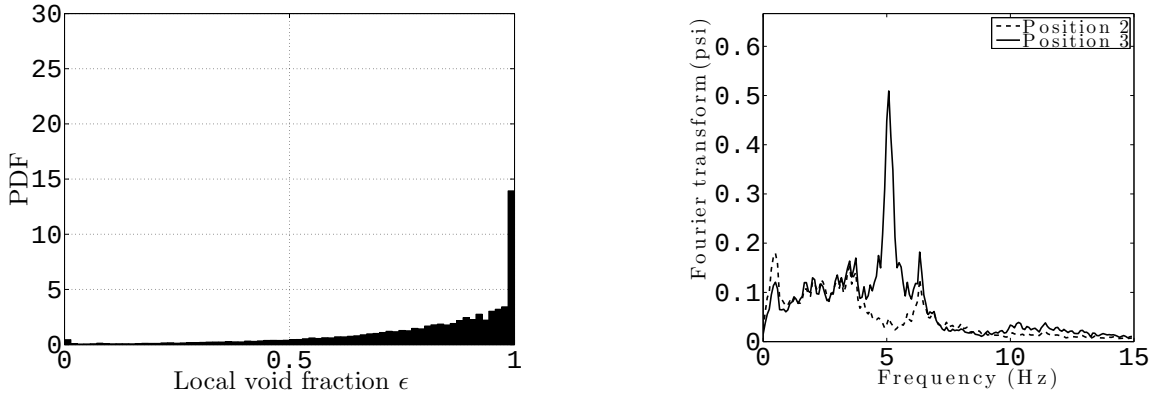

(a) Example of PDF with β=80%, U=0.9m/s and a sampling length L_s=1,9cm.

(b) Example of Fourier transform with β=96%, U=6, 9m/s .

Figure 4: Example of PDF and Fourier transform.

5. Flow pattern characteristics

The analysis of pressure and void fraction fluctuations lead to the identification of four flow patterns called annular, churn, slug and bubbly. Two subcategories of churn flows are also defined: churn-1 and churn-2. The intermittent flow is defined by the occurence of large structures of both water and air, and large pressure fluctuations. When no pressure fluctuations were discernible, but big structures of both gas and air were present, the intermittent pattern was considered in a slug flow pattern. When pressure fluctuations were detectable in addition, the intermittent pattern was considered in a churn flow pattern.

5.1. Annular flow
The two criteria used to define the annular flow rest upon the absence of pressure fluctuations [9] and the absence of water structures larger than 1 mm, which is about the maximum size of drops in annular flow [13]. The optical probe is really fragile, which prevented its use with the high gas flow rate required to observe annular flow. Thus it was only used to confirm that the flow was not annular, hence to show the occurrence of annular flow we relied on pressure measurements.

We decided to classify as flat profile any pressure Fourier transform with a maximum of less than 0.2 psi. An example of this nearly flat profile can be seen on Fig. 5, and indeed fluctuations are still visible, but is not considered as two phase flow effect.

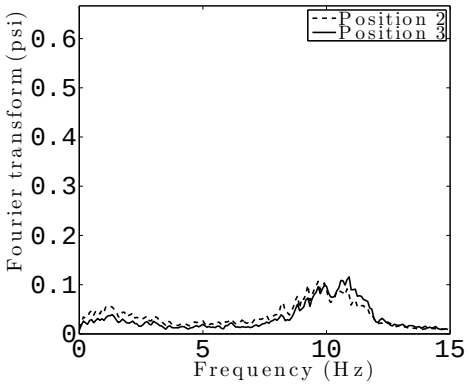

Figure 5: Fourier transform with β=98% and U=14, 4m/s.

5.2. Churn

Churn flow is defined by the presence of large structures of both water and air, and of pressure oscillations. We observed different kinds of pressure fluctuations depending on the flow parameters. For several conditions two low frequency components are detected around 0.6 Hz and 2.5 Hz. For other conditions a high frequency component is detected around 7 Hz. We then decided to separate the intermittent churn pattern in two different flow patterns: churn-1 and churn-2. All churn void fraction PDF exhibit large structures of both air and water.

5.2.1. Churn-1 The churn-1 flow pattern is defined by important low frequency oscillations. As explained above [4], those pressure fluctuations are a signal of churn flow occurrence. A typical pressure Fourier transform of churn-1 can be observed on Fig. 6a, and a typical void fraction PDF of churn-1 on Fig. 7a. Frequencies of peaks are at 0.6 Hz and 2.5 Hz and do not depend on velocities or void fraction. The sampling length for both churn PDFs was set to 1 mm, since the goal is to verify that we have water structures larger than 1 mm, indicating structures larger than drops.

5.2.2. Churn-2 In the churn-2 flow pattern, low frequency pressure oscillations are no longer observable, while high frequency pressure fluctuations are. A typical Fourier transform of churn-2 is plotted on Fig. 6b, and a typical PDF of churn-2 on Fig. 7b. The frequency of this peak linearly depends on homogeneous velocity U which allows to define a Strouhal number.

5.3. Slug flow

Slug flow pattern is characterized by large bullet shaped structures of gas. These structures are usually larger than the pipe diameter in length. Given our geometry, void fraction PDF is based on a sampling length of 1.9 cm, the minimal width of the flow path. A typical void fraction PDF with a peak showing the presence of those structures is shown on Fig. 8a. This pattern also requires water structures larger than drops, larger than 1 mm. The PDF with a sampling length of 1 mm must then exhibit a peak at ε=0% to show that there are water structures larger than 1 mm. A typical example of the PDF with this sampling length is shown on Fig. 8b. However,

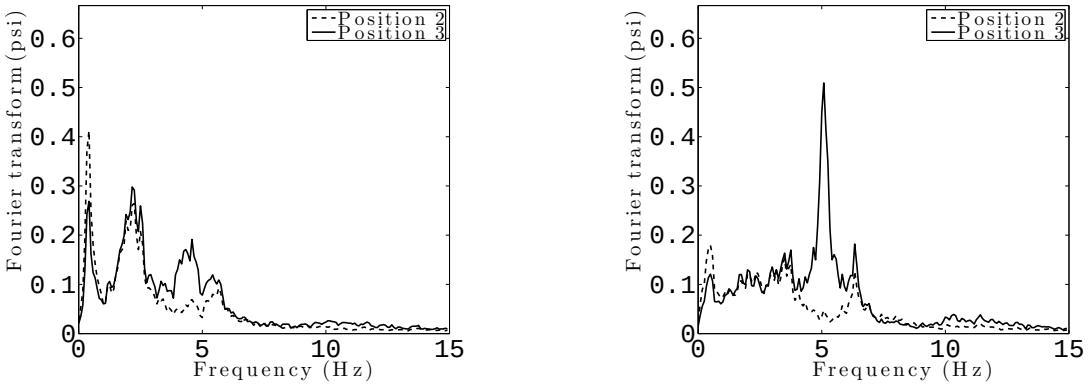

(a) Churn-1 Fourier transform with β=95%, U=8.6m/s .

(b) Churn-2 Fourier transform with β=96%, U=6.9m/s .

Figure 6: Typical Fourier transform for churn-1 and churn-2.

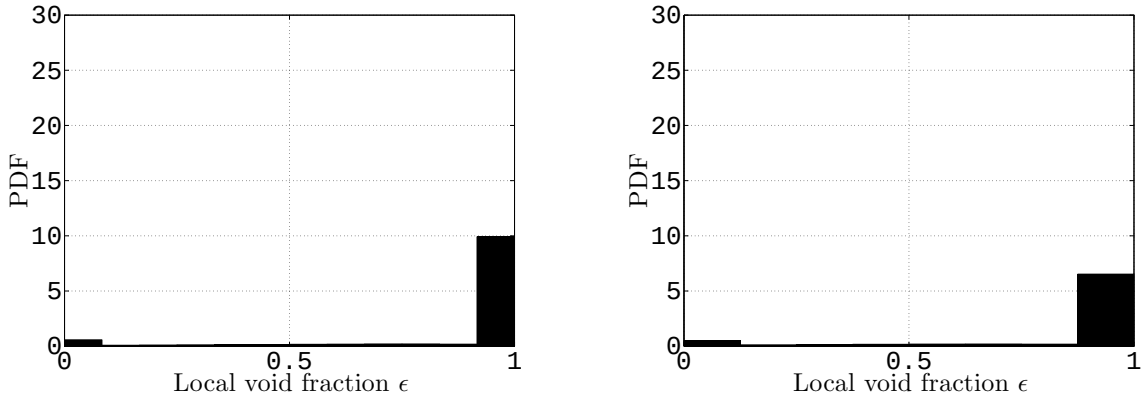

(a) Example of churn-1 PDF with β=95%, U=4.5m/s, and L_s=1mm .

(b) Example of churn-2 PDF with β=95%, U=6.3m/s, and L_s=1mm .

Figure 7: Typical PDFs for churn-1 and churn-2.

no pressure oscillations can be detected for this flow pattern which indicates the flow is of slug type.

5.4. Bubbly flow

The Fourier transform is nearly flat for bubbly flows. A bubbly flow is defined by contrast with slug flow. It is a flow pattern whose void fraction PDF exhibits no peak at ε=100% with a sampling length of 1.9 cm. A typical PDF of bubbly flow is plotted on Fig. 9a, and a typical Fourier transform on Fig. 9b.

6. Flow pattern map

Now that we characterized the various flow patterns we can define flow patterns areas on the map.

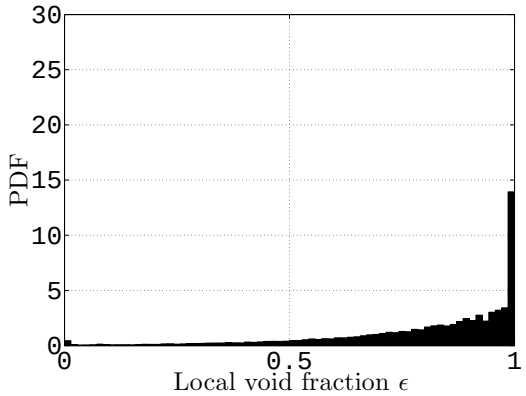

(a) PDF with β=80%, U=0.20m/s and L_s=1.9cm.

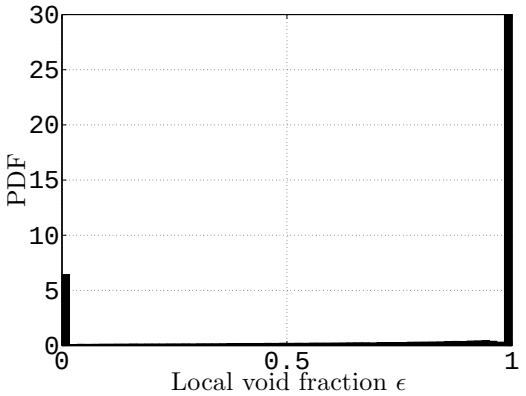

(b) PDF with β=80%, U=0.8m/s and L_s=1mm.

Figure 8: Typical PDFs for slug flow with different sampling lengths.

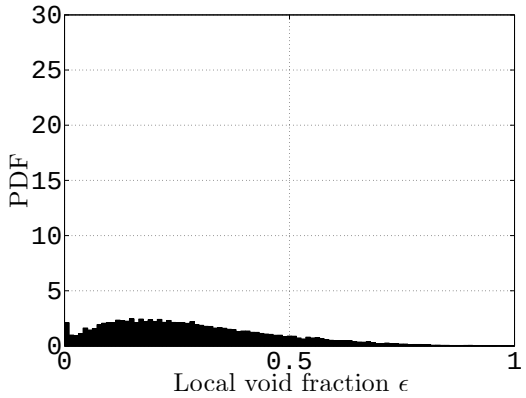

(a) Example of bubbly PDF with β=10%, U=0.6m/s and L_s=1.9cm.

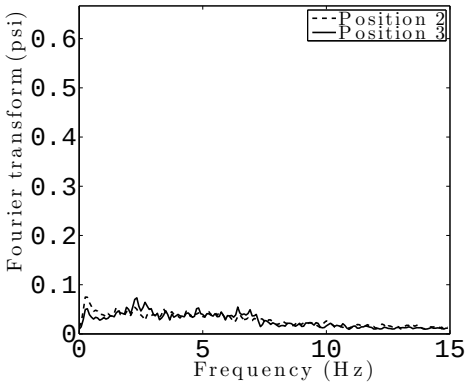

(b) Example of bubbly Fourier transform with β=60% and U=1.0m/s.

Figure 9: Typical PDF and Fourier transform for bubbly flow.

6.1. Borders obtained through the pressure analysis

The contour of maximum of Fourier transform peaks for both low frequency and high frequency oscillations is plotted on Fig. 10a. The threshold allowing to determine that a point is churn is set to 0.2 psi. We see two different zones of important pressure fluctuations that correspond to churn-1 and churn-2 areas.

6.2. Borders obtained through PDF analysis

Here we segregate cases between having air structures larger than 1.9 cm, and bubbly flow. The flow is of slug pattern when at leat 10 % of air is flowing as stuctures bigger than 1.9 cm. The resulting map is plotted in Fig. 10b

6.3. Comparison with existing maps

The different flow patterns and sample points determined in this study are compared with those in tube bundle from Noghrehkar *et al.* and from Ulbrich and Mewes on Fig. 11a. Additionally we compare our data to those of Taitel *et al.* in a different geometry that is a vertical cylindrical pipe

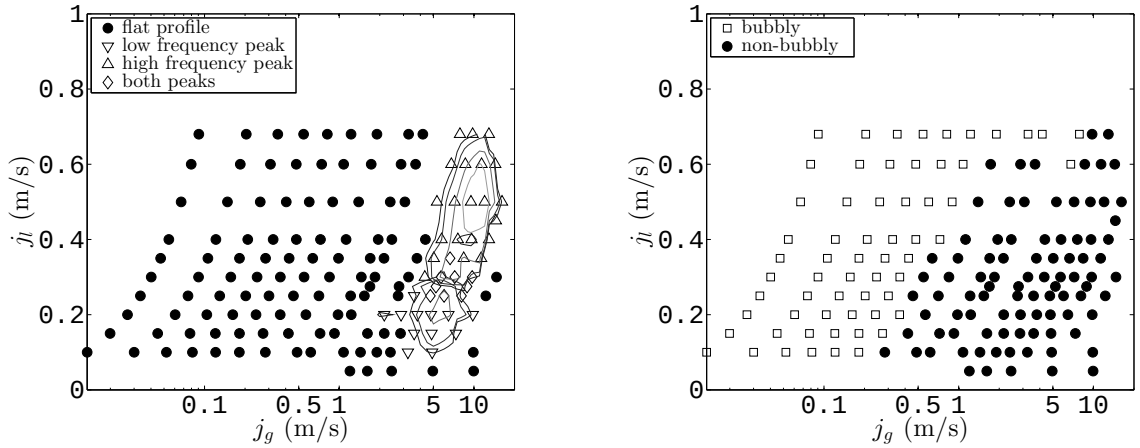

(a) Flow pattern map thanks to pressure oscillations. (b) Flow pattern map thanks to void fraction variations.

Figure 10

on Fig. 11b. With low fluid velocity, similar boundaries to those defined by Ulbrich and Mewes are obtained, even if we segregate different types of intermittent flow. However very different results for water velocities larger than 0.4 m/s are obtained. When they see only bubbly flow, we notice important pressure fluctuations, and large gas structures. Bubbly flow is obtained in the same range as Noghrehkar *et al.*, but the beginning of the annular flow is obtained for much higher gas velocities in our work. The beginning of the annular flow for them matches with the beginning of our pressure oscillations. As we explained earlier the methodology used by Noghrehkar *et al.* is not pertinent with annular flows, which explains the difference between our flow pattern map and their flow pattern map. Finally Taitel *et al.* predict a beginning of annular flow consistent with our data, but we have really different results in terms of slug and churn flows. It is not surprising since annular flow occurs when gas can carry the weight of drops. Hence the geometry should not matter a lot for the transition with annular flow. Transition from bubbly flow to intermitent flow is observed by Taitel *et al.* at lower gas flow rates than we do. The bundle is responsible for this effect since it prevents large gas structures, allowing bubbly flow at higher gas rates. Since we have tubes with larger diameters than Ulbrich and Mewes and Noghrehkar *et al.*, our present results look closer to those obtained in a pipe.

7. Conclusion

In this work new information has been brought on the flow pattern map and more precise information on the flow characteristics of each flow pattern has been produced. In particular pressure fluctuations due to two phase flow were identified. As exiting from a nozzle, the flow pattern is certainly close to an annular flow, we might expect pressure fluctuations. Indeed, as gas expands and finishes in a bubbly flow, churn flow is expected to happen in between. Further work in a more open geometry is necessary to conclude, and the methodology with the use of both an optical probe and a pressure probe will be appropriate. We also exhibited a default concerning the sampling time used in the PDF by Noghrehkar *et al.*, and proposed a better definition based on the physical understanding of two phase flows.

7.1. Acknowledgments

Authors wish to acknowledge the financial support, assistance and encouragement from the BWC/AECL/NSERC Industrial Research Chair in Fluid-Structure Interaction from

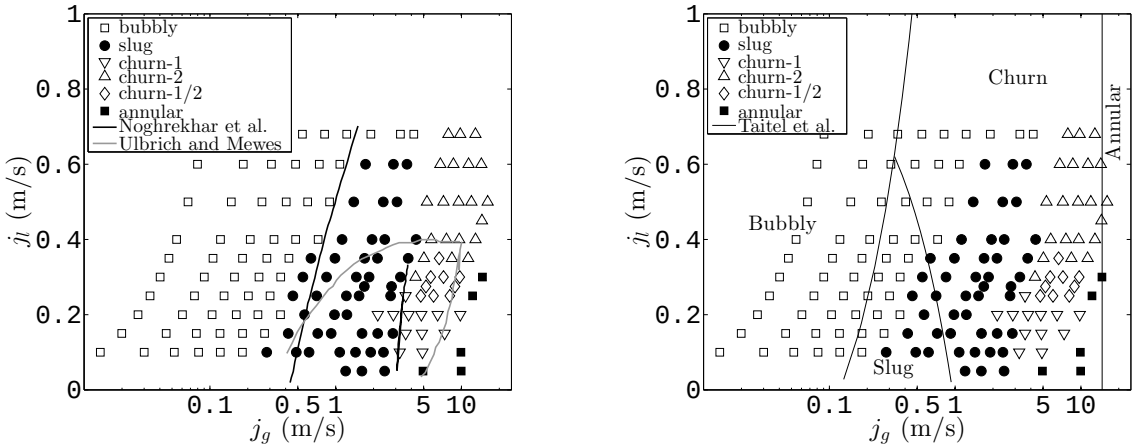

(a) Flow pattern map compared to Noghrehkar *et al.* and Ulbrich and Mewes maps.

(b) Flow pattern map compared to Taitel's maps.

Figure 11: Comparison of our results with the literature

Polytechnique Montréal, and the NSERC Individual Discovery Grant Program. Authors also wish to thank Benedict Besner for his precious support with the experimental setup.

References

[1] Noghrehkar G, Kawaji M and Chan A 1999 *International Journal of Multiphase Flow* **25** 857–874
[2] John T M A S 2013 San onofre to be permanently closed, http://www.kpbs.org/news/2013/jun/07/san-onofre-be-permanently-closed/ URL `http://www.kpbs.org/news/2013/jun/07/san-onofre-be-permanently-closed/`
[3] Syeda S R and Ansery A M 2015 *Journal of Mechanical Engineering* **44** 137–141
[4] Tapucu A 2009 The thermal-hydraulics of two-phase systems
[5] Taitel Y, Bornea D and Dukler A 1980 *AIChE Journal* **26** 345–354
[6] McQuillan K and Whalley P 1985 *International Journal of Multiphase Flow* **11** 161–175
[7] Kawahara A, Chung P Y and Kawaji M 2002 *International Journal of Multiphase Flow* **28** 1411–1435
[8] Grant I D R and Murray I 1972 *Pressure drop on the shell-side of a segmentally baffled shell-and-tube heat exchanger with vertical two-phase flow* (National Engineering Laboratory)
[9] Ulbrich R and Mewes D 1994 Vertical, upward gas-liquid two-phase flow across a tube bundle
[10] Mureithi N and Masabarakiza C 2011 *ASME 2011 Pressure Vessels and Piping Conference* (American Society of Mechanical Engineers) pp 353–364
[11] Pettigrew M, Zhang C, Mureithi N and Pamfil D 2005 *Journal of Fluids and Structures* **20** 567–575
[12] Zhang C, Pettigrew M and Mureithi N 2007 *Journal of Pressure Vessel Technology* **129** 21–27
[13] Azzopardi B 1997 *International Journal of Multiphase Flow* **23** 1–53